Feature Article . . .

EFFECT OF FERROSILICON, SILICON AND ALUMINUM ANTIOXIDANTS ON MICROSTRUCTURE AND MECHANICAL PROPERTIES OF MAGNESIA-GRAPHITE REFRACTORY

Z. A. Nemati[1], S. K. Sadrnezhaad[1], H. R. Ahmadi Mooghari[2]

[1]Center of Excellence for Advanced Processes of Production and Shaping of Materials, Department of Materials Science and Engineering, Sharif University of Technology, PO Box 11365-9466, Tehran, Iran, ***nemati@sharif.edu***

[2]Former Msc Student At Materials And Energy Research Center, PO Box 31787-316, Karaj, Iran

ABSTRACT

Effect of addition of various antioxidants such as ferrosilicon, pure silicon, aluminum and their combinations on microstructure and mechanical properties of magnesia-graphite refractories were investigated at different temperatures. Sample preparation and measurements were according to DIN or ASTM standards. The data showed that up to about 1300°C, the slope of the apparent porosity against temperature of the samples was positive; but lower than that of the samples containing no antioxidant. Effect of the carbothermal reduction of MgO became significant only at temperatures greater than 1400°C. At 750 to 1000°C, the CCS and MOR of the specimens without any antioxidant decreased with temperature. The depth of the decarburization layers and the percentage of the oxidation surface increased with temperature, no matter the sample contained or did not contain ferrosilicon or silicon aluminum combination. Oxidation resistance of the samples containing ferrosilicon-silicon was greater than that of the ferrosilicon or silicon containing specimens. Results indicated that the worst hydration condition was with the samples containing aluminum. Other samples showed a good resistance against hydration. Best results were obtained with the samples containing (a) 1-3 wt% silicon, (b) 2-4 wt% ferrosilicon and (c) 4% ferrosilicon plus 1% Al.

1. INTRODUCTION

MgO-C bricks are utilized in various metallurgical furnaces such as BOF converters, LF vessels and EAF units. They are especially used in high capacity steelmaking systems such as UHP arc melting furnaces. MgO-C bricks have desirable properties such as resistance to spalling, thermal shock and corrosion [1-3]. Their carbon content decreases, however, due to oxidation. Further enhancements in durability of these bricks are, therefore, hardly achievable.

Due to the weak bonding between MgO and graphite, some kind of chemical or ceramic bonding is required to improve the mechanical properties and performance of these refractory materials. Graphite oxidation results in property degradation and lifetime shortening of the MgO-C refractory materials. This process causes structural bonding deterioration and excess porosity formation which eliminates the beneficial effects attributed to the presence of graphite within the matrix [4-5]. These problems can be remedied by engineering of chemical formula, using of proper raw materials and performance of suitable heat treatments.

Previous studies have shown that addition of a low temperature carbon containing material (such as pitch or resin) or a high temperature ceramic phase (such as an oxide, a carbide or a boride) [6-13] improves the properties of the MgO-C bricks. Reducing materials such as Al, Si and Al-Mg powders as well as carbides, borides, and complex B_4C, ZrB_2, SiB_6, TiB_2, BN, CaB_6, Al_4SiC_4, Mg B_2O_6 and $Al_8B_4C_7$ compounds are generally added to MgO-C refractories in order to suppress their oxidation rate. A great deal of research has been conducted, during recent years, on influence of the antioxidants and their role in increasing the life time of the MgO-C bricks. These studies show that the added antioxidants act differently during their industrial application.

Thermodynamic studies conducted by different groups such as Yu and Yamaguchi [14], Goto et al. [15], Poirier and Rigaud [16] and many others [17-18] have been focused on the effect of various additives. Zhang et al. [19] have studied, for example, the effect of Al, Si and B_4C. They have concluded that ceramic phases form from 1200 to 1500°C in this system. Their investigations have also shown that Al_4C_3 and AlN form at low temperatures and Al_2O_3 and MA phases form at high temperatures in a system that contains Al as an antioxidant [20-21]. SiC, Si_3N_4, SiO_2 and M_2S phases form similarly in a system containing the Si and/or SiC antioxidant [21-22].

Different additives have different absorption potentials for oxygen. It is reported that each antioxidant has a specific range of oxygen absorption [23]. For metallic materials, it is in the range of 30-53%, for borides, it is in the range of 42-54% and for carbides, it is in the range of 39-70% [23].

An important issue is the kinetics of oxidation. Numerous authors have considered kinetic modeling of gas-solid reactions [24-26] as applied to the refractory-graphite oxidation reactions. Examples are Rigaud et al. [27,31], Faghihi and Yamaguchi [28], Ghosh et al. [10,29], Rongti et al. [30] and Hashemi el al. [32] who have studied the oxidation kinetics of MgO-C refractories. Many others have

also addressed the oxidation kinetics of MgO-C refractories [33-37]. An important issue is the influence of the additives on the mechanical properties of the MgO-C bricks that must further be treated.

Effect of addition of antioxidants is not, however, studied comprehensively yet. An antioxidant such as ferrosilicon has, for example, some beneficial effects on properties of the magnesia-graphite refractories. There is not, however, significant information available in the literature about it. Ferrosilicon can be used as an antioxidant, too. Its addition to the refractory increases the oxidation resistance of the MgO-C refractory. Both species contained in the MgO-C refractory, i.e. silicon (Si) and iron (Fe), exhibit good potential for absorption of oxygen. A combination of ferrosilicon, silicon and aluminum could also be added to the MgO-C refractory. This combination seems to be more effective than each single one. This paper presents the most recent findings on the effect of the combined as well as the individually added ferrosilicon, silicon and aluminum antioxidants into the MgO-C refractories.

2. EXPERIMENTAL PROCEDURE

The samples were made of 97% pure Chinese sintered magnesia. Size distribution of the magnesia grains is shown in **Table 1.** Two main characteristics of this material are high MgO content and C/S >2. Natural Chinese graphite flakes with an ash content of 3.3 wt% were added to the magnesia grains together with 4 wt% of liquid phenol (Novalac resin) to produce the refractory samples required for the tests. After mixing the raw materials, the samples were formed under 120 -140 MPa by hydraulic press and were heated at 240°C for 18 hrs. The samples were prepared based on DIN or ASTM standards in order to eligibly perform MOR, CCS, density and apparent porosity measurements on them.

Three antioxidant raw materials were used: Ferrosilicon (F.S.), Silicon (Industrial grade) and Aluminum (Fluka grade). Chemical composition and physical properties of the raw materials are listed in **Tables 2-6.** Ferrosilicon was domestic. Its XRD pattern and relevant Fe-Si phase diagram are shown in **Figures 1-2.** The samples were fired in a bed of coke at 750, 1000, 1300 and 1600°C, for 5 hrs. For oxidation test, tempered samples with 50x50x70 mm size were maintained at 1000, 1300 and 1600°C for 2 hrs under atmospheric air. Taking the ratio of the black surface to the total surface and the depth of decarburization into account, the oxidation resistance was then evaluated. Hydration tests were conducted under humidity of 98% at 50°C for 142 hrs on the samples having 20x40x20 mm dimensions. Hydration resistance of the samples was determined both before and after the tests.

Different combinations of the raw materials used in this study are given in **Table 7.** XRD analysis was used to determine the phases formed in the samples. Since the amounts of the antioxidants in some samples were lower than the detection range of the XRD analysis, a few samples were made with higher amounts of antiox-

Table 1. Size distribution of MgO grains.

Size (mm)	3-5	2-3	0.1-2	< 0.1
Concentration (%)	22.5	14.2	49.2	14.1

Table 2. Chemical analysis and density of the sintered Chinese magnesia.

	MgO	CaO	SiO_2	Al_2O3	Fe_2O_3	LOI
Concentration (%)	97.1	1.26	0.56	0.09	0.89	0.01
Density (g/cm^3)	3.51					

Table 3. Physical properties of the Chinese flaky graphite.

Content	Wt %
Carbon	95.17
Moisture	0.02
Volatile material	1.6
Ash	3.3

Table 4. Chemical analysis of graphite ash.

Total Fe	K_2O	Na_2O	CaO	MgO	Al_2O_3	SiO_2	Chemical Composition
17.81	1.37	0.79	5.06	7.67	17.10	50.20	Wt %

Table 5. Chemical analysis of phenolic resin (Novalac).

Property	Amount	Optimum value
pH	7.05	8-9
Percent of Solid Resin	62.6 %	63 – 80 %
Density at 20°C	1.21 (gr/cm^3)	> 1.15
Viscosity	> 10	min 10
Remained Carbon	42.64	> 40 %
Color	No color	No color
Free Phenol	1 %	< 1 %

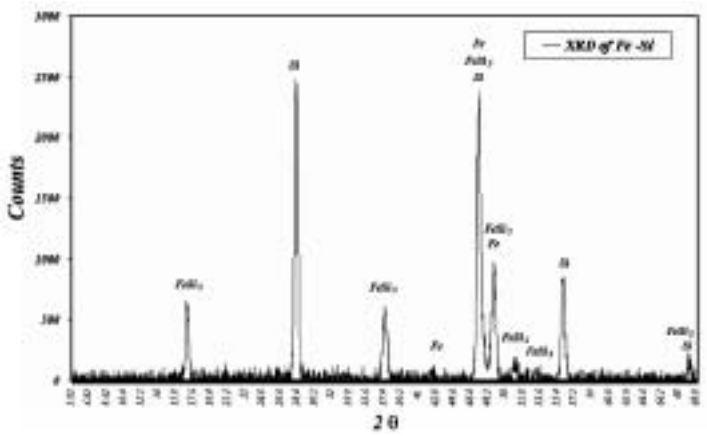

Figure 1. XRD pattern of ferrosilicon.

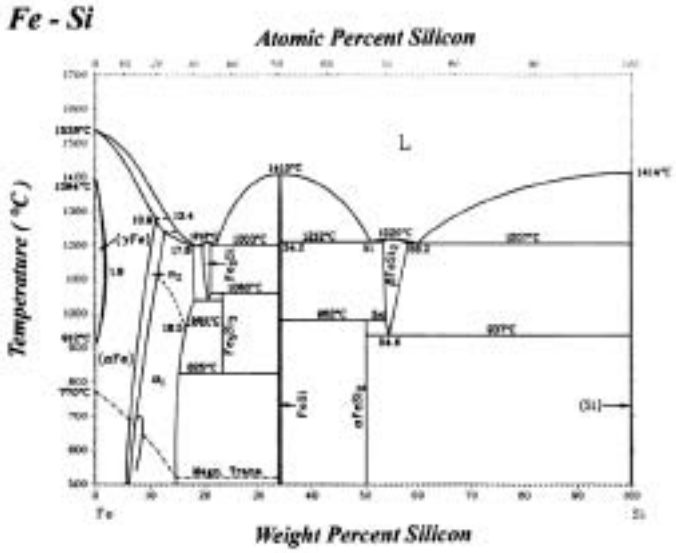

Figure 2. Phase diagram of Fe-Si.

Table 6. Chemical analysis of antioxidants.

Na	*Fe*	*Ti*	*Mn*	*Ca*	*Mg*	*Si*	*Al*	Chemical Composition
----	0.27	Trace	Trace	0.1	Trace	0.35	99.18	Wt % (Al)
----	0.62	Trace	------	<0.1	Trace	99.1	Trace	Wt % (Si)
<0.01	25.3	<0.1	-----	1.39	0.1	71.85	1.04	Wt % (F.S.)

Table 7. Purity of the raw materials and composition of the samples.

		Sample Code							
Raw Materials	Purity	00	S0[1]	S1	S3	S5	A1	A3	A5
Sintered Magnesia	97 % MgO	0.85	0.85	0.85	0.85	0.85	0.85	0.85	0.85
Flake Graphite	95 % C	0.15	0.15	0.15	0.15	0.15	0.15	0.15	0.15
Phenolic Resin	-	0.4	0.4	0.4	0.4	0.4	0.4	0.4	0.4
Aluminum Powder	99 % > Al	0	0	0	0	0	1	3	5
Silicon Powder	99 % > Si	0	0	1	3	5	0	0	0
Ferrosilicon Powder	71.85 % Si 25.3 % Fe	0	5	4	2	0	4	2	0

[1] S0 = A0, Both samples are the same and has only ferrosilicon

Table 8. Chemical composition of samples prepared for XRD analysis.

Sample Code / Raw Materials	00	A15	S15	FS15	FSA36	FSS36
Sintered Magnesia	0.85	0.85	0.85	0.85	0.85	0.85
Flake Graphite	0.15	0.15	0.15	0.15	0.15	0.15
Phenolic Resin	0.4	0.4	0.4	0.4	0.4	0.4
Aluminum Powder	0	0.15	0	0	0.24	0
Silicon Powder	0	0	0.15	0	0	0.24
Ferrosilicon Powder	0	0	0	0.15	0.16	0.16

idants merely for phase detection purposes. The compositions of these samples are shown in **Table 8.**

3. RESULTS AND DISCUSSION

Density and porosity of the samples

Bulk density and apparent porosity of the samples coded 00 after tempering at 240°C and heating at 600°C were measured according to ASTM C-20 in oil. The Data are shown in **Table 9.**

Figure 3 shows that the apparent porosity of the samples increases with temperature, no matter they contain any ferrosilicon, silicon or they do not. It can be seen that the apparent porosity of the samples containing these antioxidants increases with a slower slope than that of the samples containing no antioxidant at temperatures less than 1300°C. Based on this figure, the S1 and S3 samples have the least apparent porosities.

Porosity changes are caused by three processes that occur during the firing of the specimens: (a) loss of volatile materials, (b) reduction of oxide-impurities and (c) oxidation of the residual carbon. It seems that the carbothermal reduction of MgO becomes significant at temperatures higher than 1400°C.

Table 9. Bulk density and apparent porosity of samples after tempering at 240°C and heating at 600°C.

Properties		Sample (00) with 10 wt%G
Bulk density after tempering	(g/cm^3)	2.88
Apparent porosity after tempering	(%)	7.86
Bulk density after heating at 600°C	(g/cm^3)	2.85
Apparent porosity after heating at 600°	(%)	12.10

According to **Figures 3-4**, the rates of the change of the apparent porosities of the samples depend on the type of the antioxidants. This is due to the formation of carbide and oxide phases, volume expansion of the phases and filling up of the pores with products of the Si, Al and Fe reactions.

It seems that the formation of forsterite, magnesioferrite, carbide and oxide phases at temperatures above 1100°C (for samples containing Al) and above 1300°C (for samples containing Si) cause the decrease of the apparent porosity. This result is similar to that mentioned by previous researchers [7-15]. In samples containing Fe, iron carbide is formed by the following reaction:

$$3Fe(s) + C(s) \rightarrow Fe_3C(s)$$

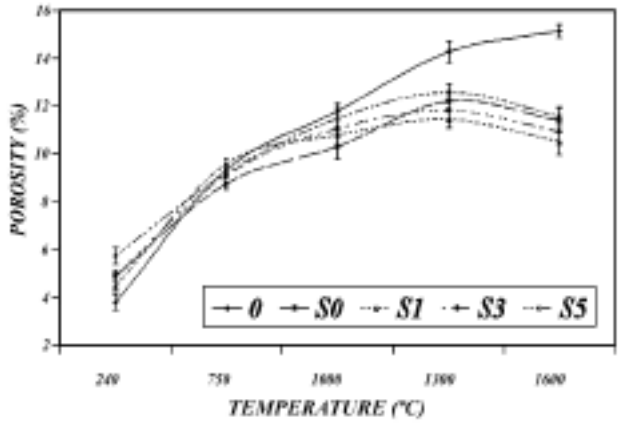

Figure 3. Apparent porosity of Si-FeSi as a function of firing temperature.

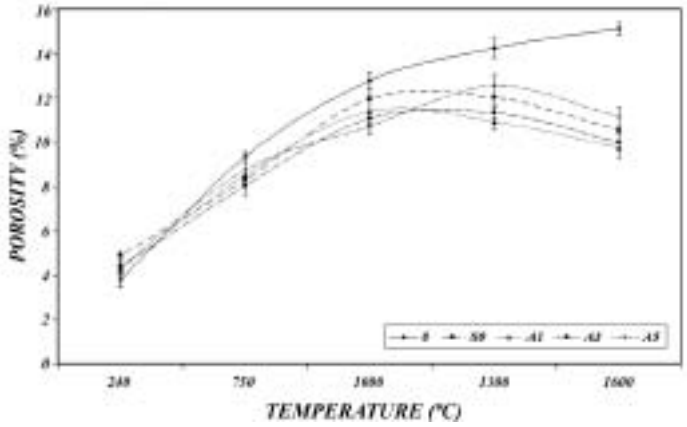

Figure 4. Apparent porosity of Al-FeSi as a function of firing temperature.

magnesioferrite is then formed from reaction of carbide with the oxide materials present in the sample according to an unknown mechanism. Specimens containing both ferrosilicon and silicon have, thus, less apparent porosity than the others. Less apparent porosity of the samples S1 and S3 may also be due to the volume expansion of the phases formed such as forsterite and magnesioferrite. The difference in samples S1 and S3 might be due to the Fe and Si contents of the samples. The SEM images are shown in **Figures 13-16.**

Mechanical properties (CCS and MOR) of the Specimens

Results of CCS and MOR tests of the samples containing ferrosilicon and silicon (FeSi-Si) are shown in **Figures 5-6**, respectively. The CCS and MOR of the specimens without antioxidants decrease with temperature. The CCS and MOR of specimens with antioxidant decrease with temperature up to 1000°C. This behavior is, however, different above 1000°C where samples with antioxidants increased in strength at 1600ºC and S3 have more CCS and MOR than S0 and S5.

Results of CCS and MOR tests on samples containing ferrosilicon and aluminum are shown in **Figures 7-8**, respectively. CCS and MOR of the specimens without antioxidant decrease with temperature. CCS and MOR of the specimen with antioxidant decrease with temperature up to 750-1000°C and then increase with temperature at higher temperatures.

Up to 750-1000°C, CCS and MOR of the samples depend on pyrolysis of the resin and oxidation of the residual carbon. This behavior is, however, different above those temperatures. The formation of such phases as forsterite, magnesioferrite and carbides increases ceramic binding and improves the mechanical properties of the refractory material. It is mentioned that the carbothermal reduction of MgO above 1300°C may have some improving effects. CCS and MOR of S1 and S3 specimens are better than S0 and S5 specimens. The formation of magnesoferrite and forsterite cause more binding between system components in S1 and S3 specimens. As the firing temperature increases, the quantities of these compositions increase, too. Ceramic binding between system components consequently increases and causes more MOR and CCS developments. Ferrosilicon and silicon containing specimens

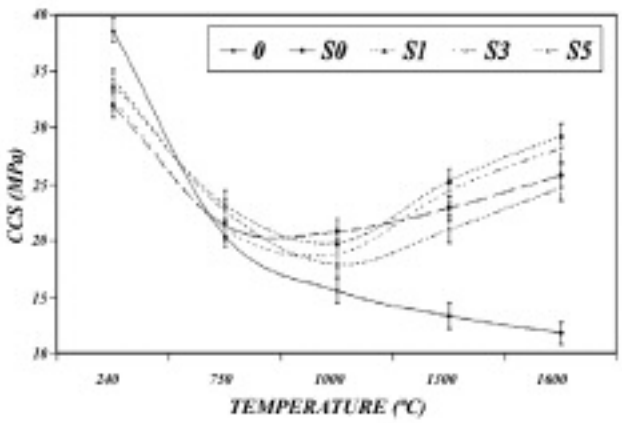

Figure 5. CCS of samples with FeSi-Si as a function of firing temperature.

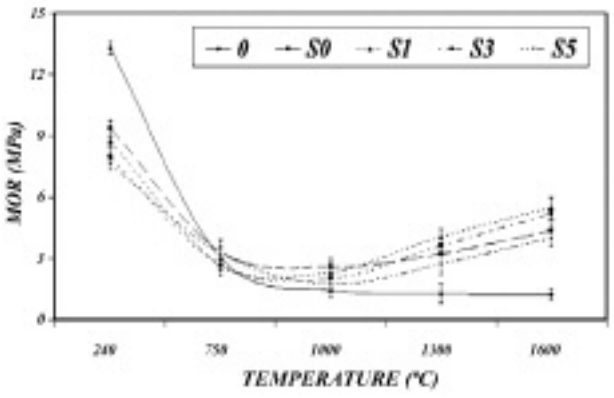

Figure 6. MOR of samples with FeSi-Si as a function of firing temperature.

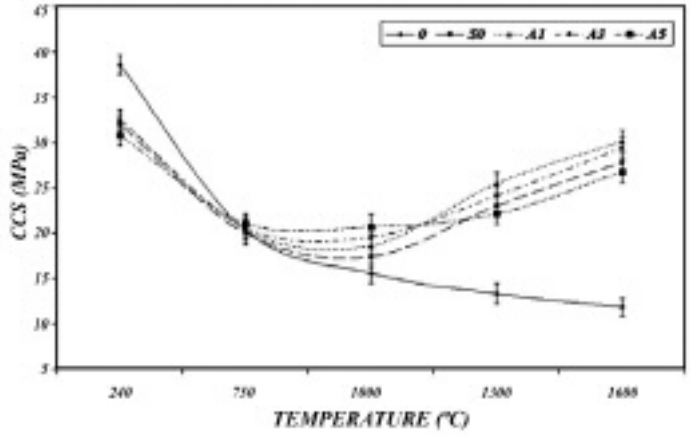

Figure 7. CCS of samples with Al-FeSi as a function of firing temperature.

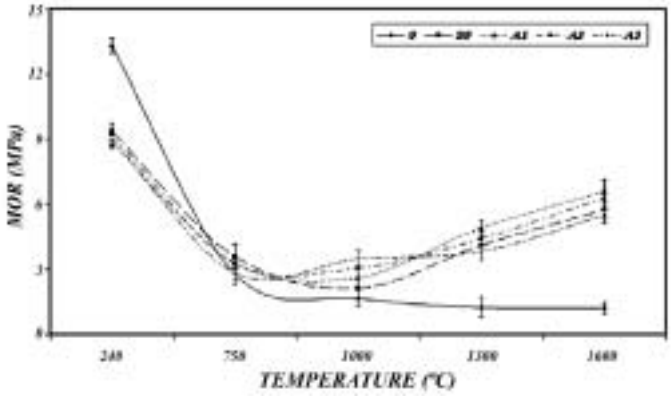

Figure 8. MOR of samples with Al-FeSi as a function of firing temperature.

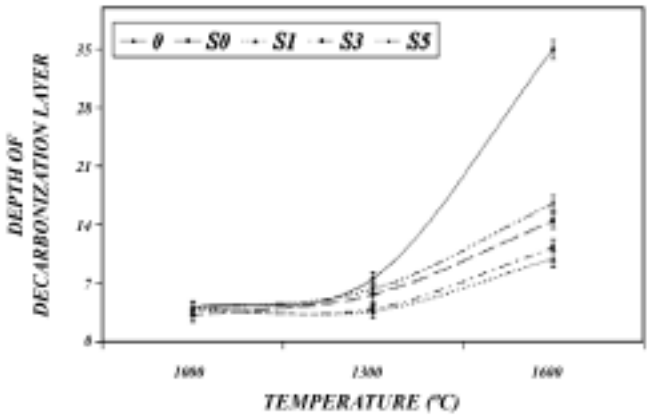

Figure 9. Depth of decarburization layer of the samples with and without ferrosilicon and silicon as a function of firing temperature.

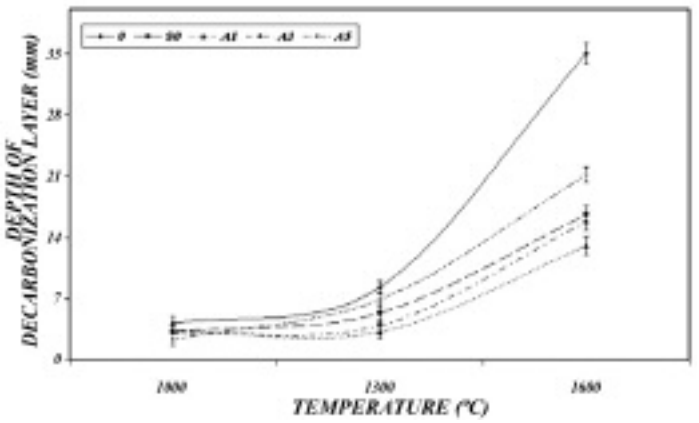

Figure 11. Depth of the decarburization layer of the samples with and without ferrosilicon and aluminum as a function of the firing temperature.

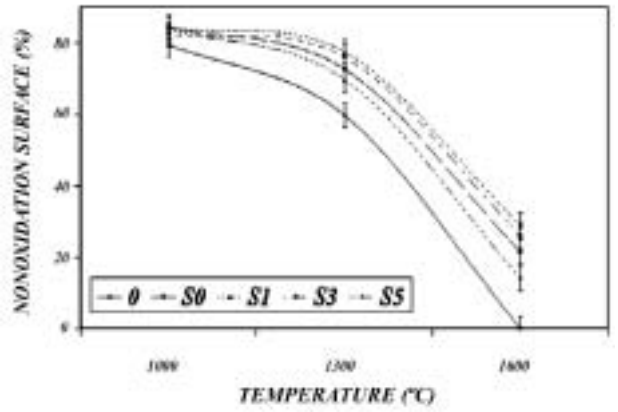

Figure 10. Non-oxidation surface of the samples with and without ferrosilicon and silicon as a function of firing temperature.

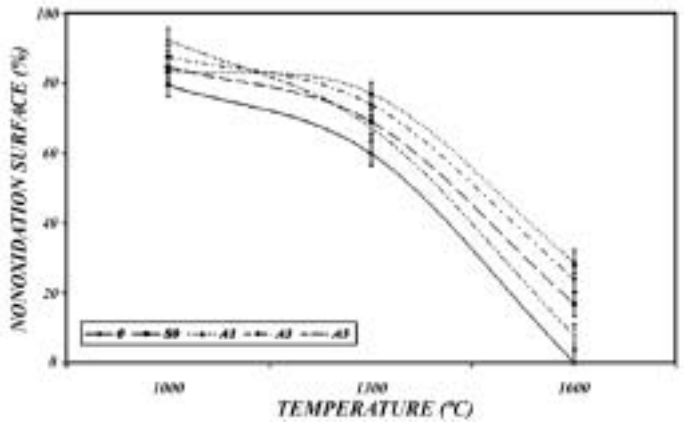

Figure 12. Non-oxidation surface of the samples with and without ferrosilicon and aluminum as a function of firing temperature.

have greater MOR and CCS. The SEM image are shown in **Figures 13-16.**

Oxidation Resistance of Specimens

Results of oxidation of the samples with and without ferrosilicon, silicon and aluminum are shown in **Figures 9-10.** The data indicates that the depth of the decarburization layer and the percentage of the oxidation surface increase with temperature. The range of these changes is more palpable at temperatures greater than 1300°C.

Similar behavior was observed in the samples with and without ferrosilicon and aluminum. The data indicates that as the temperature increases, the depth of the decarburization layer and the percentage of the oxidation surface increases as shown in **Figures 11-12.**

Previous studies show that the oxidation of carbon is controlled by pore diffusion mechanism [32]. Oxygen must pass through the porous layer formed on the exterior layer of the refractory material. This process is rather rapid in samples without antioxidant. It seems that resistance to the oxidation of the specimens decreases with porosity. Formation of such phases as forsterite and magnesioferrite in specimens S1 and S3 above 1300°C causes volume expansion and improves densification of the sample. It tightens, therefore, the microstructure and improves oxidation properties. These processes fill up the pores and improve the oxidation resistance of S1 and S3 specimens at 1600°C, particularly. Many researchers believe that silicon reacts with carbon and forms SiC at low temperatures. It then changes to SiO_2 due to oxidation. The consequence is the filling up of the pores [27-32].

Hydration of the samples

The hydration resistance of the samples conducted under the conditions mentioned previously are shown in the **Table 10.** Worst results were obtained for the samples containing aluminum. Other samples showed good resistance against hydration. Samples A1, A3 and A5 showed undesirable hydration resistance:

$$Al_4C_3 + 12H_2O \Leftrightarrow 4Al(OH)_3 + 3CH_4$$

Based on the literature [33], it is believed that the formation of Al_4C_3 and subsequent reaction with moisture and formation of $Al(OH)_3$ and its expansion are the main reasons behind this phenomenon. Formation of these phases is discussed next.

SEM analysis of the material

Different mechanisms are proposed to explain the effects of silicon and aluminum on formation of different phases such as SiC, SiO_2, Al_4C_3 and Al_2O_3, Forsterite and $MgAl_2O_4$ [6-17]. Results of phase analyses showed formation of spinel at 1300°C and 1600°C. The SEM image of the spinel at 1600°C is shown in **Figure 14**.

The sample S5 was heated at 1300°C for 5 hours. SiC was formed under this condition. **Figure 13** shows the SEM image of the SiC

Table 10. Hydration resistance of the samples.

Temperature (°C)			
1600	1300	1000	Sample Code
Grade A	Grade A	Grade A	00
Grade A	Grade A	Grade A	S0
Grade A	Grade A	Grade A	S1
Grade A	Grade A	Grade A	S3
Grade A	Grade A	Grade A	S5
Grade B	Grade B	Grade B	A1
Grade B	Grade B	Grade C	A3
Grade C	Grade D	Grade F	A5

Grade A = no hydration, Grade B = little hydration,
Grade C = medium hydration,
Grade D = high hydration, Grade F = very high hydration

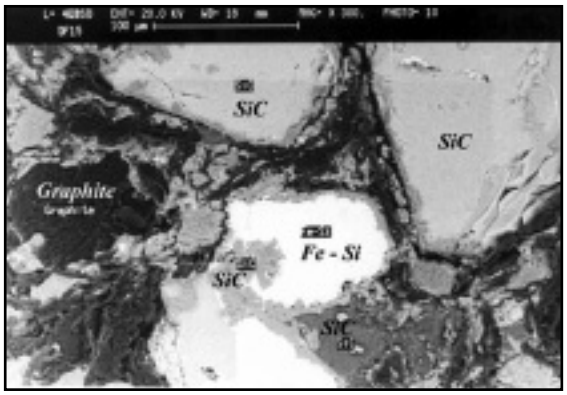

Figure 13. SEM image of SiC and unreacted ferrosilicon phases in S5 sample heated at 1300°C for 5 hr.

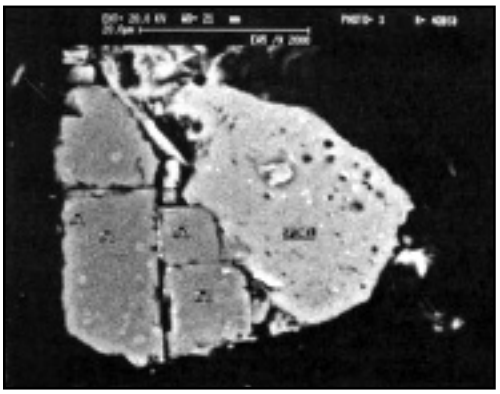

Figure 14. SEM image of the spinel formed at 1600°C.

produced and the ferrosilicon remained un-reacted in the sample. EDAX analyses of the SiC and the un-reacted ferrosilicon confirmed the chemistry of these phases.

The results obtained shows that by increasing temperature, the phase Forsterite ($2MgO•SiO_2$) forms in vicinity of the phase SiC, at 1600°C. SEM and X-ray spectroscopy analyses approve the formation of Forsterite in-between magnesia particles of the refractory as shown in **Figure 15.**

There is no information available in the literature on the mechanism and effect of iron as an antioxidant present in the MgO-C refractories. A mechanism similar to that of the Al and Si antioxidants may be proposed for iron. It seems that Fe_3C phase is formed at 1000°C and 1300°C. Fe_3C is then changed to magnesioferrite ($MgO•Fe_2O_3$) at 1600°C as shown in **Figure 16**. The mechanism

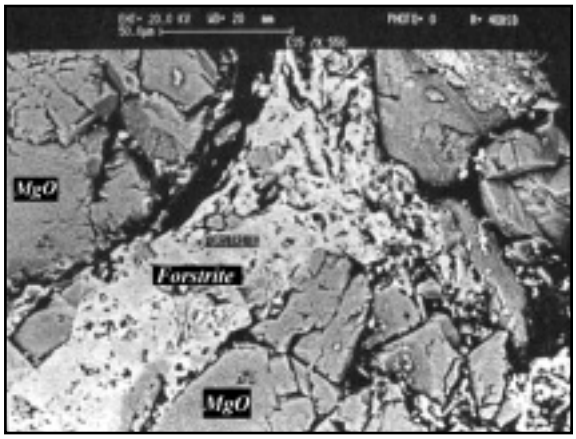

Figure 15. SEM image of Forsterite phase at 1600ºC in S5 sample.

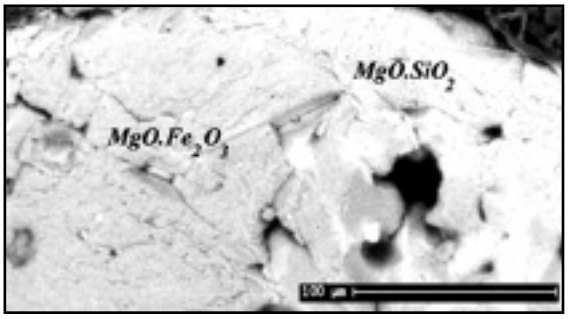

Figure 16. SEM picture of Magnesoferrite and Forsterite.

for this process is unknown. At high temperatures, the analysis shows that the spinel phase is also formed in the system.

XRD analysis of the formed phases in the systems

XRD showed that when sample A15 was heated from 1000°C to 1600°C, Al_4C_3 and $MgO•Al_2O_3$ were formed in the system. The other formed phase in the system is listed in each pattern.

5. SUMMARY

Effects of ferrosilicon, silicon and aluminum added to MgO-Graphite refractory have been investigated in this research. The main conclusions are:

Apparent porosity of the samples containing the antioxidants increased with slow slope up to 1100-1300°C. It seems that the formation of forsterite, magnesioferrite and carbide and oxide phases might cause the decreases in the apparent porosity. It seems that the carbothermal reduction of MgO signifies only at high temperatures; i.e. T ≥1400°C.

The CCS and MOR of specimen without antioxidants decrease with temperature below 750 to 1000°C. They are related to pyrolysis of the resin and the oxidation of the residual carbon. This trend changes above 1000°C. The formation of a ceramic phase increases the ceramic binding and improves the mechanical properties of the specimen. It is also mentioned that the carbothermal reduction of MgO above 1300°C may have some effects.

The experimental data shows that in the samples with and without ferrosilicon, silicon and aluminum, the depth of decarburization layer and percentage of oxidation surface increases with temperature. Oxidation resistance of the ferrosilicon-silicon containing samples was greater than the specimens containing individual silicon or ferrosilicon species. It seems that decreasing of the porosity of the samples increases the oxidation resistance of the

specimens. The latter arises from volume expansion of new phases.

Regarding the hydration resistance, the worst results were obtained for the samples containing aluminum. Other samples showed good resistance against hydration.

The data show that there is an optimum level of ferrosilicon, silicon and aluminum in the samples. Best results were obtained for samples containing (a) 1-3 wt% silicon and 2-4 wt%. ferrosilicon, (b) ferrosilicon and silicon and (c) ferrosilicon and aluminum. Optimum data was obtained from samples containing 1% Al and 4% ferrosilicon.

ACKNOWLEDGMENT

The authors gratefully acknowledge A. Agheaei and R. Yazdanirad of Materials and Energy Research Center (MERC), H. Paydar and M. Poya-mehr of Azar Refractories Company Research Center and Ceramic Group at Sharif University of Technology.

REFERENCES

1. H. Shikano, "Refractories Handbook," The Technical Association of Refractories, Japan, (1998) pp. 170-182.
2. M. Rigaud and Z. Ningsheng, "Major Trends in Refractories Industry at the Beginning of the 21st Century," *China's Refractories*, **11**[2] 2002.
3. M. Rigaud, "Forecasting the Future of the Refractories Industry: the Real Challenges that Must be Faced Over the Next Ten Years," World Refractory Congress-Suntec Singapore 02-04 June 2002.
4. L. A. Zamboni and R. E. Caligaris, "Different Compositions of MgO-C Bricks Used in Ladle Slag Line," UNITECR'97, vol. II, 765-773.
5. Y. Hoshiyama et al., "Environment Friendly MgO-C Products with Non-phenol Resin," UNITECR'97, vol. II, 1199-806.
6. A. Yamaguchi, K. Inoue and S. Hashimoto, "Synthesis, Sintering and Properties of Al_4SiC_4," UNITECR, Congress, pp.1349-56 (2001).
7. L. Hongxia, "Synthesis of New Composite Anti-Oxidants and Their Application to Carbon Containing Refractories," *China's Refractories*, **9**[2] 3-6 (2000).
8. C. Baudin, C. Alvarez and R. E. Moore, "Influence of Chemical Reaction in Magnesia-Graphite Refractories: II, Effects of Aluminum and Graphite Content in Generic Products," *J. Am. Ceram. Soc.,* **82**[12] 3539-48 (1999).
9. S. Zhang, N. J. Marriott and W. E. Lee, "Thermo Chemistry and Microstructures of MgO-C Refractories Containing Various Antioxidants," *J. Eur. Ceram. Soc.,* 21[8] 1037-1047 (2001).
10. N. K. Ghosh, D. N. Ghosh and K. P. Jagannathan, "Oxidation Mechanism of MgO-C in Air at Various Temperatures," *Br. Ceram. Trans. J.,* **99**[3] 124-128 (2000).
11. N. K. Ghosh, K. P. Jagannathan and D. N. Ghosh, "Oxidation of Magnesia-Carbon Refractories with Addition of Aluminum and Silicon in Air," *Interceram,* **50**[3] 196-202 (2001).
12. A. Yamaguchi, S. Zhang and J. Y U .S. Hashimoto, "Behavior of Antioxidants Added to Carbon-Containing Refractories," UNITECR'97, Congress, 341-318.
13. Z. A. Nemati, and M.R. Vassalam, "The Effects of Metallic Anti-oxidants in MgO-C Refractories," UNITECR'01 Congress, 2001.
14. Yu and Yamaguchi, *J. Ceram. Soc. Jpn,* **101**[4] 475-479 (1993).
15. Goto et. al. [14], *J. Am. Ceram. Soc.*, **80**[2] 3461-71 (1997).
16. J. Poirier and M. Rigaud, *J. Can. Ceram. Soc.,* **62**[1] 370-76 (1993).
17. H. Li, J. Yu and K. Hiragushi, "Synthesis of New Ceramic Composite Powders and Their Use as Anti-Oxidants in Carbon Containing Refractories," UNITECR'01, Congress, 1476-82.
18. Zhang et. al, *J. Eurp. Ceram. Soc.,* **21**[8] 1037-1047 (2001).
19. R. J. Sarkinen and J. J. Harkki, "Thermodynamic Calculations of Reactions Inside MgO-C Antioxidant Linings," UNITECR'97, Congress, 755-763.
20. K. Ichikawa, H. Nishio, O. Nomura and Y. Hoshiyama, "Suppression Effects of Aluminum on Oxidation of MgO-C Bricks," *Taikabutsu Overseas,* **15**[2] (1995).
21. S. Uchida and K. Ichikawa, "High Temperature Properties of Unburned MgO-C Brick Containing Al and Si Powders," *J. Am. Ceram. Soc.,* **81**[11] 2910-16(1998).
22. T. Shouxin and C. Zhaoyou, "The Mechanism of Silicon and Silicon Carbide Making Carbon Containing Materials Antioxidize," *China's Refractories,* **5**[4] (1996).
23. P. Bartha and G. Weibel, "Outlook for Synthetic Resin Bonded Magnesia Graphite Bricks," Proceeding of International Symp. CIM, 45-57, 1996.
24. V. L. Lou, T.E. Mitchell and A. H. Heuer, "Graphical Displays of the Thermodynamics of High-Temperature Gas-Solid Reactions and Their Application to Oxidation of Metals and Evaporation of Oxides," *J. Am. Ceram. Soc.,* **68**[2] 49-58 (1985).
25. S. Hiroyuki and K. Masayasu, "Oxidation Kinetics of Magnesia-Carbon Refractories," 44th International Colloquium on Refractories, Aachen, pp. 52-54 (2001).
26. S. K. Sadrnezhaad, A. Gharavi and A. Namazi, "Software for Kinetic Process Simulation," IJE Transactions A: Basics **16**[1] 61-72 (2003).
27. M. Rigaud, C. Richmond and P. Bombard, "Oxidation Kinetics of Graphite in Basic Refractory Composites," UNITECR'91, p. 266
28. M. A.Faghihi-Sani and A. Yamaguchi, "Oxidation Kinetics of MgO-C Refractory Bricks," *Ceramics International,* **28**[8]835-839 (2002).
29. N.K. Ghosh, K.P. Jagannathan and D.N. Ghosh, "Oxidation of Magnesia-Carbon Refractories with Addition of Aluminum and Silicon in Air," *Interceram,* **50**[3] (2001).
30. Rontgi et al, "Kinetics of Reduction of Magnesia with Carbon," Thermochimica Acta 390, 2002, P.P. 145-151
31. X. Li, M. Rigaud and S. Palco, "Oxidation Kinetics of Graphite Phase in Magnesia-Carbon Refractories," *J. Am. Ceram. Soc.,* **78**[4] 965-71 (1995).
32. Z. A. Nemati, K. Sadrnezhaad, and B. Hashemi, "Oxidation Mechanism in MgO-C Refractories," Tehran International Refractory Conf., 2004, Tehran, Iran.
33. O. Benhui, W. Ruikun and W. Zhongxian, "The Effects of Non-Metal Additives on Hydration Resistance of MgO-C Bricks," *China's Refractories,* **9**[1] 29-31 (2000).
34. N. C. Lubaba, et al., "Microstructure and Strength of MgO-Carbon Composite Refractory Materials," *Br. Ceram. Trans. J.,* **88**[2]47-54 (1989).
35. S. A. Franklin, and B. J. S. Tucker, "Hot Strength, and Thermal Shock Resistance of Magnesia-Carbon Refractories," *Br. Ceram. Trars. J.*, **94**[4] 151-156 (1995).
36. J. M. Robin, et al., "Thermomechanical Behavior of Magnesia-Carbon Refractories," *Br. Ceram. Trans. J,.* **94**[1] 1-10 (1998).
37. C. Baudin, C. Alvarez and R. E. Moore, "Influence of Chemical Reactions in Magnesia- Graphite Refractories: I, Effects On Texture and High-Temperature Mechanical Properties," *J. Am. Ceram. Soc.*, **82**[12] 3429-38 (1999). RAM